JOC The Journal of Organic Chemistry

Article

pubs.acs.org/joc

Rules for the Design of Highly Fluorescent Nucleoside Probes: 8-(Substituted Cinnamyl)-Adenosine Analogues

Lital Zilbershtein-Shklanovsky, Michal Weitman, Dan Thomas Major, and Bilha Fischer*

Department of Chemistry, Gonda-Goldschmied Medical Research Center and the Lise-Meitner-Minerva Center of Computational Quantum Chemistry, Bar-Ilan University, Ramat-Gan 52900, Israel

Supporting Information

ABSTRACT: Currently, there are no tools that can help the design of useful fluorescent analogues. Hence, we synthesized a series of 8-(substituted cinnamyl)-adenosine analogues, **5**−**17**, and established a relationship between their structure and fluorescence properties. We attempted to find a correlation between maximum emission wavelengths (λ_{em}) of **5**−**17** or their quantum yields (φ), and Hammett constants (σ_p and σ_m) of the substituent on the cinnamyl moiety. A linear correlation was observed at low-medium σ values, but not at high σ values (≥0.7). Next, we explored correlation between λ_{em} and φ of **5**−**17** and computed HOMO and LUMO energy levels of fragments of **5**−**17**, i.e., 8-vinyl 9-Me-adenine (fluorescent molecule), **18**, and substituted toluene rings (fluoresence modulators), **19**−**30**. High φ correlated with relatively close LUMO levels of **19**−**30** and **18** (−0.076 to −0.003 eV). The electron density of LUMO of nitro analogues **9** and **15** is localized on the aryl ring only, which explains their low φ. Calculation of HOMO−LUMO gap of **5**−**17** enables accurate prediction of the λ_{abs} for a planned analogue, and LUMO levels of an aryl moiety vs 8-vinyl 9-Me-adenine, allows the prediction of high or low φ. These findings lay the ground for prediction of fluorescence properties of additional analogues having a similar structure.

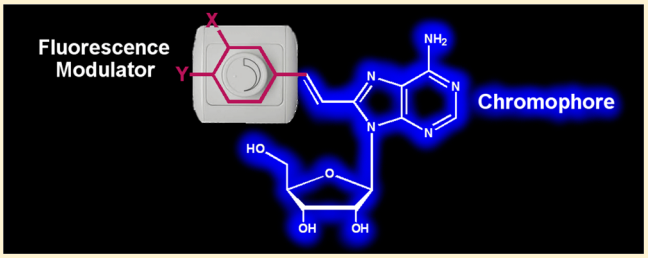

INTRODUCTION

Fluorescent organic molecules constitute an important class of compounds in many fields of science and are widely used as biological imaging probes, sensors, and light emitting devices, as well as for identification and quantification of nucleic acids.[1−4] For the latter application, natural nucleotides are not useful as fluorescent probes because of their extremely low quantum yields.[5−7] Hence, the use of extrinsic probes, namely, fluorescent dyes, is necessary.[8−11] These dyes are used for detecting genetic material in DNA microarrays,[12] fluorescent in situ hybridization (FISH),[13] gels,[14] and cells, by fluorescence microscopy or electrophoresed gels.[15]

However, commonly used fluorescent dyes suffer from various limitations. For instance, most dye molecules are large and hydrophobic and have limited water solubility. In addition the large dye molecule attached to a nucleotide alters the efficiency of enzymatic incorporation into DNA/RNA, resulting in different levels of labeling and prohibits quantification of nucleic acids.

Because of limitations and complications of the current methodologies applying extrinsic dyes, the development of useful fluorescent nucleosides has been a subject of intensive research. Over the past decade a number of nucleoside analogues with intrinsic fluorescence, replacing natural DNA bases in oligonucleotide probes, have been reported as an alternative to dye-substituted nucleosides.[16−18] Thus, the fluorescent properties of the natural nucleosides were significantly improved by extending the purine/pyrimidine π-system.[19−22]

For example, extending the purine π-system by C8 modifications, e.g., 8-vinyl-adenosine, **1**, results in a longer emission wavelength and higher quantum yield as compared to adenosine (λ_{em} 388 nm; φ 0.66 vs λ_{em} 319 nm; φ 0.00026).[23,24]

Another example is the extension of adenine chromophore at C2,N3-positions to give N^2,N3-etheno-adenosine, **2**, exhibiting improved fluorescence characteristics (λ_{em} 420 nm; φ 0.03).[25,26]

Fluorescent pyrimidine nucleosides include pyrrolo-C, **3**, φ 0.04, and the pyrrolo-dC, **4**, φ 0.05, analogues, which maintain a proper Watson−Crick H-bonding. These analogues were incorporated into an oligonucleotide; however, their quantum yields decreased upon incorporation and were quenched even further upon duplex formation (Figure 1).[27]

Previously, we have designed and synthesized fluorescent purine nucleoside probes based on a minimal extension of the nonfluorescent adenosine or guanosine chromophore.[28] In these nucleoside analogues, the purine C8-position was conjugated either directly, or through an alkenyl or alkynyl linker, to an aryl/hetero aryl moiety to determine the effect of the type of linker on fluorescence. Moreover, the influence of the type of the substituent on the aryl moiety, i.e., electron-donating-group (EDG) vs electron-withdrawing-group (EWG)

Received: September 15, 2013
Published: November 8, 2013

 © 2013 American Chemical Society

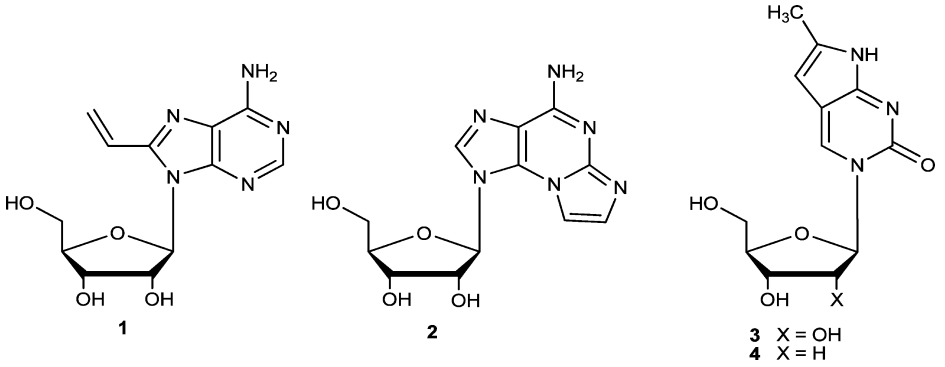

Figure 1. Fluorescent purine and pyrimidine analogues: 8-vinyladenosine, **1**; C2,N3-etheno-adenosine, **2**; Pyrrolo-C, **3**; Pyrrolo-dC, **4**.

on fluorescence and the effect of number of substituents were studied as well. These extensions of the natural purine nucleobases at the C-8 position significantly enhanced their spectral properties. For instance, the emission wavelength of the natural adenosine was red-shifted by 36−140 nm, and the quantum yield increased 10−3100-fold. In particular, alkenyl conjugated nucleoside analogues (e.g., **5**) displayed the longest shift of emission wavelengths (75−140 nm) vs parent nucleosides. However, the quantum yields of alkenyl conjugated analogues were either very high for several analogues (e.g., φ 0.81, for analogue **5**), or very low for others (e.g., φ 0.005, for analogue **6**), Figure 2. These contradictory

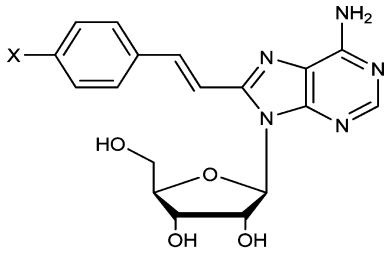

Figure 2. Example of previously studied analogues, **5** and **6**.

data led us to extend our research and to establish a relationship between the probes' structure and their fluorescence properties, with a view to setting rules for prediction of improved fluorescent nucleoside probes.

Although there are numerous reports on the structural dependence of fluorescence properties,[29−31] i.e., λ_{em} and φ values, there are no clear rules that can help predict fluorescence characteristics of a molecule based on its chemical structure.

Previous attempts at finding a relationship between the fluorescent characteristics of several organic compounds such as *N*-hexyl-1,8-naphthalimides,[32] 7-hydroxycumarins,[33] and benzofurazan[34] and sigma Hammett constants revealed an excellent correlation, which enabled the prediction of the fluorescent characteristics of additional analogues. However, these predictions are specific to the studied structure and cannot be used for predicting fluorescence of nucleoside analogues.

We targeted the establishment of the relationship between the chemical nature of the substituents on the cinnamyl moiety and fluorescence characteristics of the resulting C-8-cinnamyl nucleoside analogues **5**−**17**.

Specifically, we report on the synthesis and spectral characterization of a series of 8-(cinnamyl)-modified adenosine analogues **5**−**17** (data for analogues **5**, **6**, and **8** were previously reported),[28] Figure 3. We explored a possible correlation between maximum emission wavelengths or quantum yields and Hammett constants (σ_p and σ_m) of the substituent on the cinnamyl moiety.

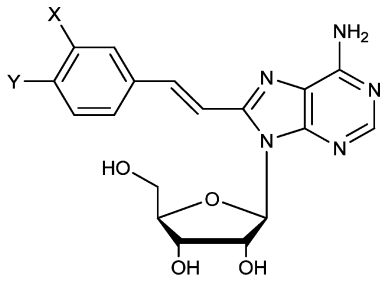

5: X = H Y = CF_3
6: X = H Y = OMe
7: X = H Y = H
8: X = H Y = F
9: X = H Y = NO_2
10: X = H Y = CN
11: X = H Y = COOMe
12: X = H Y = Me
13: X = F Y = H
14: X = CF_3 Y = H
15: X = NO_2 Y = H
16: X = CN Y = H
17: X = CF_3 Y = CN

Figure 3. 8-(Cinnamyl)-adenosine analogues synthesized and studied here.

In addition, we explored the correlation between the fluorescence properties of **5**−**17** and calculated HOMO and LUMO energy levels of 8-(substituted cinnamyl)-9-Me-adenine analogues, or their fragments: 8-vinyl 9-Me-adenine, **18**, and variously substituted toluene analogues, **19**−**31** (Figure 4).

RESULTS

Selection of a Set of Adenosine Analogues for Establishing Rules for Prediction of Fluorescent Nucleoside Analogues. Previously, we have reported the large enhancement (up to 162-fold) of the quantum yield of 8-cinnamyl-adenosine analogues triggered by the *p*-substituent on the aryl group (*p*-CF_3, F, or OMe, instead of H).[28]

Here, we explored the fluorescence of a series of 8-cinnamyl-adenosine analogues representing a wider chemical space (analogues **5**−**17**).

We have designed and synthesized a series of 8-cinnamyl adenosine analogues bearing various substituents at *p*- or *m*-position of the aryl moiety. Selection of the substituents was done on the basis of their Hammett substituent constants, σ_p

dx.doi.org/10.1021/jo402050x | J. Org. Chem. 2013, 78, 11999−12008

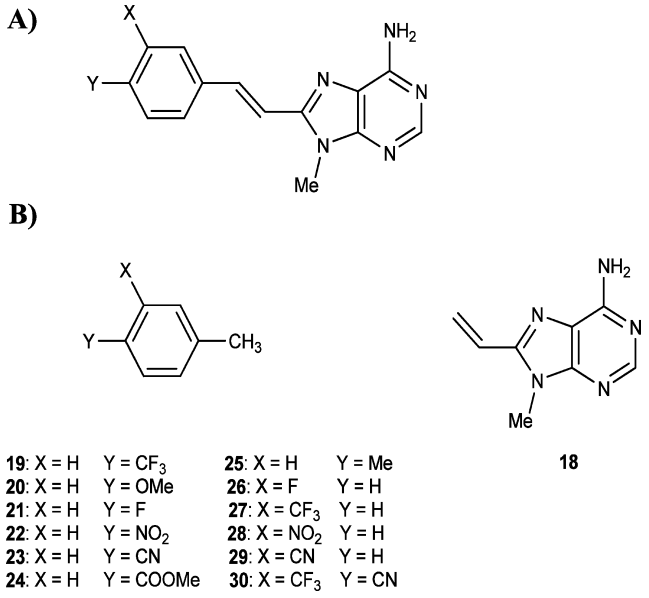

Figure 4. 8-(Substituted cinnamyl)-9-Me-adenine analogues for which spectral properties and HOMO–LUMO energies were calculated. (A) 8-(Substituted cinnamyl)-9-Me-adenine analogues studied here. (B) 8-(Substituted cinnamyl)-9-Me-adenine constituents studied here: 8-vinyl 9-Me-adenine, **18**, and substituted toluene rings, **19**–**30**.

and σ_m, to achieve the widest possible range of σ values. Hammett constants are based on dissociation of benzoic acid and *p*/*m*-substituted benzoic acids. The sigma values are derived from the equation below:

$$\sigma_x = \log(K_x/K_0)$$

where σ_x is the sigma constant for substituent *x*, K_0 is the acid dissociation constant for the ionization of benzoic acid and K_x is the acid dissociation constant for the ionization of a substituted benzoic acid with a given substituent (*x*) at a given position on the aromatic ring.

The fluorescent analogues were designed as push–pull molecules that undergo an intramolecular charge transfer (ICT).[35,36] ICT process from the donor to the acceptor via a linker results in a large dipole moment in the excited state compared to that of the ground state; therefore, the excited state is more stabilized by the polar solvents, and the excited-state energy is lowered, resulting in longer emission wavelengths.[37−39]

Push–pull molecules are generally composed of three moieties: an electron donor (D, an electron rich aryl group); an electron acceptor (A, an electron poor aryl moiety), and an electron rich linker, which is a double/triple bond or a single bond. Since the electron-donating or -accepting character of one moiety in push–pull molecules is relative to the other moiety, the purine moiety can play either the acceptor or the donor role. In our previous results, we observed a dramatic enhancement of fluorescence when the purine moiety and the aryl group played the donor and acceptor role, respectively, by adding EWG substituents on the aryl moiety.[28]

We have applied the Suzuki–Miyuara coupling[40,41] for the preparation of analogues **5**–**8** and **12**–**13** and the Heck coupling[42] for the preparation of analogues **9**–**11** and **14**–**17**. The great advantage of these procedures is that no protecting groups are needed, thus allowing a single step reaction toward the desired conjugated nucleoside analogues. Specifically, for the Suzuki–Miyuara coupling 8-Br-adenosine[43] was directly conjugated with the appropriate boronic acid in the presence of Na_2CO_3 and a water-soluble catalytic system consisting of $Pd(OAc)_2$:P(*m*-$C_6H_4SO_3Na)_3$, in water–acetonitrile (2:1) at ∼100 °C. Products **5**–**8** and **12**–**13** were obtained in 30–35% yield upon silica gel chromatography.

For Heck coupling, 8-vinyl adenosine[44] was directly conjugated with the appropriate aryl iodide/bromide in the presence of Et_3N, $Pd(OAc)_2$, and P(*o*-tol)$_3$, in DMF at 100–105 °C. Products **9**–**11** and **14**–**17** were obtained in 10–47% yield upon silica gel chromatography.

Fluorescence Characteristics of Analogues 5–17. Maximum excitation and maximum emission wavelengths of compounds **5**–**17** were measured in a methanolic solution, and fluorescence quantum yields were determined compared to quinine sulfate in 0.1 M H_2SO_4 (λ_{ex} 350 nm, λ_{em} 446 nm, φ 0.54).[45] The concentrations of the samples were within the linear range in which the Beer–Lambert law applies, and the optical density (OD) was less than 0.05 to avoid the inner filter effect.[46] The fluorescence properties of the analogues are summarized in Table 1, and their fluorescence intensity and normalized fluorescence are presented in Figure 5.

The highest quantum yields were obtained for analogues **5**/**10** and **14**/**16** bearing a CF_3 or CN group at either *para* or *meta* position (φ: 0.81, 0.61, 0.55, and 0.66, respectively) and

Table 1. Fluorescent Properties of Analogues 5–17 in MeOH Using Quinine Sulfate As a Standard

			Hamett constant					
analogue	Y	X	σ_p[47]	σ_m[47]	λ_{ex} (nm)	ε (M^{-1} cm^{-1})	λ_{em} (nm)	φ_F
5	CF_3	H	0.54	0	340	25300	439	0.81
6	OCH_3	H	−0.27	0	345	26100	394, 419	0.005
7	H	H	0	0	336	20610	422	0.026
8	F	H	0.06	0	333	21550	436	0.025
9	NO_2	H	0.78	0	367	26450	445	0.002
10	CN	H	0.66	0	350	21180	463	0.61
11	COOMe	H	0.43[48]	0	342	24560	469	0.56
12	CH_3	H	−0.17	0	338	23920	437	0.004
13	H	F	0	0.34	336	21350	428	0.28
14	H	CF_3	0	0.43	334	23180	432	0.55
15	H	NO_2	0	0.71	335	26170	420	0.002
16	H	CN	0	0.56	337	23600	435	0.66
17	CN	CF_3	0.66	0.43	356	22680	494	0.45

dx.doi.org/10.1021/jo402050x | J. Org. Chem. 2013, 78, 11999–12008

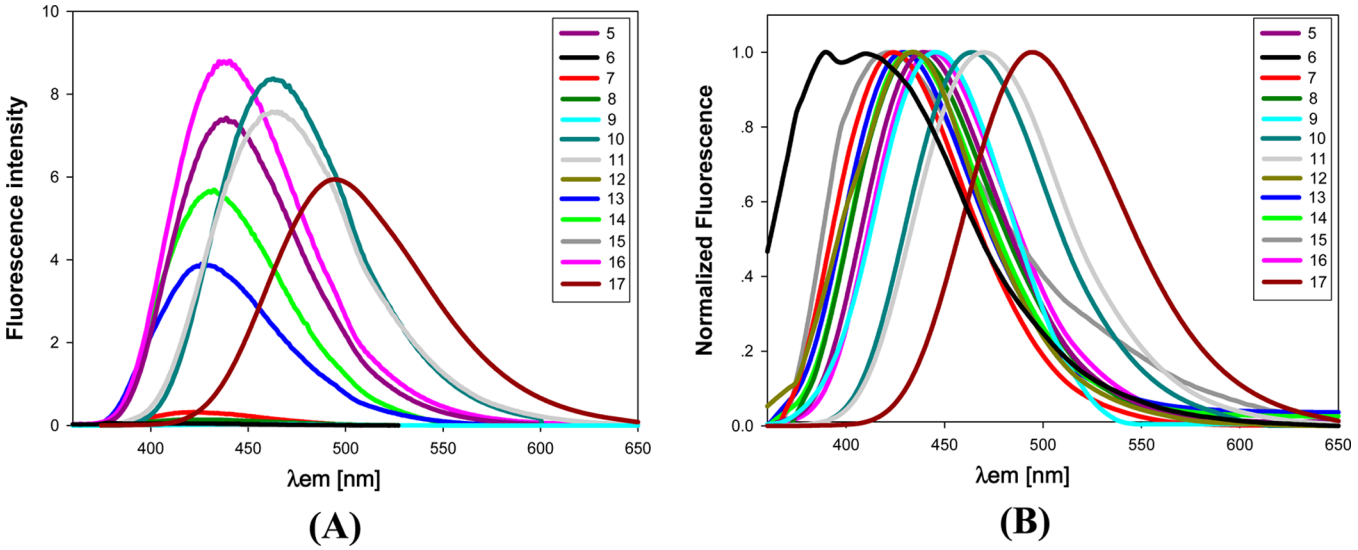

Figure 5. Fluorescence spectra (A) and normalized fluorescence spectra (B) of analogues **5**−**17** in MeOH. The concentrations of all the samples were 2−2.5 μM, and the OD was adjusted to 0.05.

for analogue **11** bearing a COOMe substituent at the *para* position (φ: 0.56). On the contrary, the lowest quantum yields were obtained for analogues with a NO_2 substituent at either the *para* or the *meta* position, with quantum yield of 0.002 for each analogue. Likewise, analogues **6** and **12** with an electron-donating group, OMe or Me, respectively, at the *para* position exhibited quantum yields of 0.005 and 0.004, respectively. Surprisingly, no additive effect was observed for analogue **17** bearing CN and CF_3 at the *para* and *meta* positions, respectively, showing a lower quantum yield, 0.45, than analogues with only CN or CF_3 (φ 0.61 and 0.55, respectively). We have observed more than one emission band in the emission spectrum of analogue **6**. This phenomenon probably occurs due to vibrational progressions.[28]

We attempted to analyze the substituent-dependent fluorescence of analogues **5**−**17**, by seeking first correlation with σ values of the substituents.

A plot of φ values vs σ_p or σ_m values, and a plot of λ_{em} values vs σ_p or σ_m values for analogues **5**−**16**, are presented in Figure 6A and 6B, respectively. As observed from Figure 6A there is a parabolic dependence between the φ values and σ_p values, with the exception of analogues **6** and **12**, having negative σ_p values. In addition, a linear dependence is observed between the φ values and σ_m values. The nitro substituted derivatives (**9** and **15**) are outliers to the general behavior (see Discussion below).

Figure 6B shows that there is no clear dependence of λ_{em} on σ_p; however, λ_{em} of analogues substituted at the *meta* position exhibited a linear dependence on σ_m, with the exception of *m*-nitro analogue **15**.

The longest λ_{em} was observed for analogue **17** (494 nm) bearing EWGs at both *para* and *meta* positions.

Theoretical Modeling. Since no clear correlation was found between φ or λ_{em} and σ_p/σ_m values of substituents of the nucleosides' aryl moiety, we concluded that parameters affecting electronically only part of the molecule are not useful for the prediction of novel highly fluorescent analogues based on 8-cinnamyl adenosine scaffold. Alternatively, we considered molecular properties of analogues **5**−**17** and explored a possible correlation between φ or λ_{em} and HOMO−LUMO energy gap.[49] HOMO and LUMO orbital energies were calculated for the ground state. Since the ribose group is not part of the fluorophore excitation and emission process, we simplified the structure and used a methyl group instead of a ribose group.

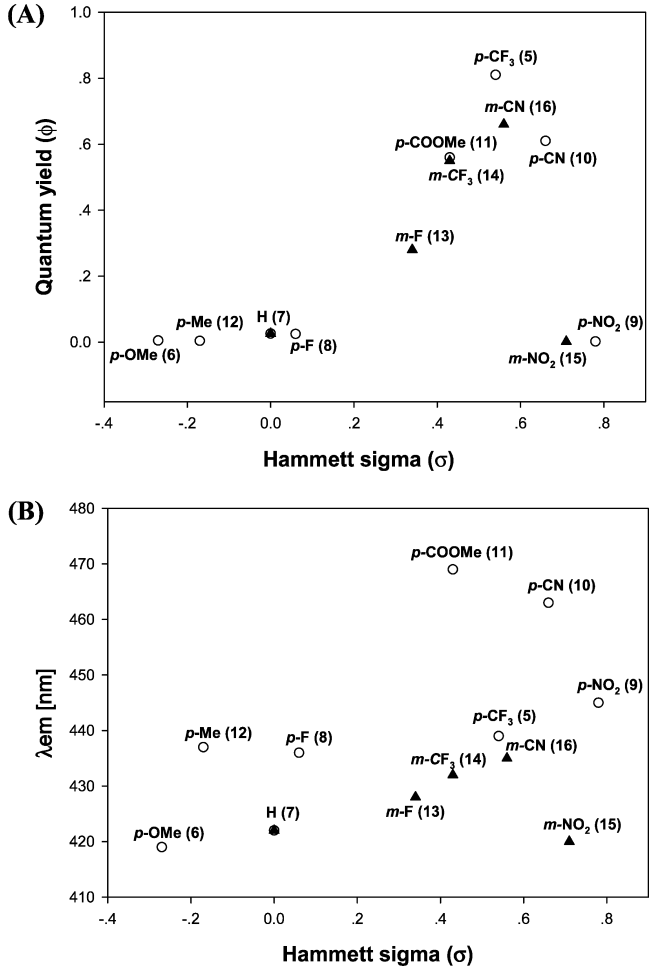

Figure 6. Dependence of φ values of adenosine analogues **5**−**16** on σ_p (○) and σ_m (▲) values (A). Dependence of λ_{em} of adenosine analogues **5**−**16** on σ_p (○) and σ_m (▲) values (B).

dx.doi.org/10.1021/jo402050x | J. Org. Chem. 2013, 78, 11999−12008

Table 2. Absorption Wavelengths (λ), Oscillator Strengths (f), Molecular Orbital Energies, and Molecular Orbital Energy Gaps of Compounds 5−17, Obtained from Calculations Run at the M062X/6-311++G(d,p) Level

analogue	substituent	λ_{abs} (nm) exp	λ_{abs} (nm) calc	f	HOMO (eV)	LUMO (eV)	Δ (eV)	φ
5	*p*-CF_3	340	332	1.08	−0.266	−0.058	0.208	0.81
6	*p*-OMe	345	334	1.24	−0.254	−0.045	0.209	0.005
7	H	336	328	1.07	−0.261	−0.050	0.211	0.26
8	*p*-F	333	328	1.06	−0.261	−0.049	0.212	0.025
9	*p*-NO_2	367	365	1.12	−0.268	−0.083	0.185	0.002
10	*p*-CN	350	346	1.21	−0.266	−0.067	0.199	0.61
11	*p*-COOMe	342	344	1.23	−0.265	−0.064	0.201	0.56
12	*p*-Me	338	330	1.18	−0.258	−0.048	0.210	0.004
13	*m*-F	336	330	1.05	−0.264	−0.054	0.210	0.28
14	*m*-CF_3	334	329	1.04	−0.265	−0.056	0.209	0.55
15	*m*-NO_2	335	341	0.70	−0.266	−0.074	0.192	0.002
16	*m*-CN	337	333	1.01	−0.266	−0.059	0.207	0.66
17	*p*-CN, *m*-CF_3	356	358	1.15	−0.269	−0.077	0.192	0.45

The experimental and computed absorption wavelengths are presented in Table 2 along with the energy of HOMO and LUMO orbitals for compounds **5**−**17**. In general, absorbance is related to the gap between HOMO and LUMO levels, and indeed the electronic transition obtained from the TD DFT calculations are mainly composed of HOMO → LUMO transition (Table S27, Supporting Information), but additional excitations also contribute to the first excited state. The oscillator strengths suggest that these are allowed transitions.

The energies of HOMO and LUMO of most substituted 8-cinnamyl-adenosine compounds are lower than that of the parent compound, **7**, with the exception of the *p*-OMe and the *p*-Me substituted compounds (analogues **6** and **12**), which have slightly higher frontier orbital energies, and F-substituted compounds (analogues **8** and **13**), which are similar to the parent compound.

The HOMO−LUMO energy gap of the parent compound, **7**, is 0.211 eV. In all compounds with electron-withdrawing groups the HOMO−LUMO gap is similar or lower than that of the parent compound. The *p*-nitro-compound, **9**, is at the extreme low end of energy gap with a value of 0.185 eV. The excellent agreement found between the calculated and the experimental absorption wavelengths validated the approach used for further calculations.

To gain further insight into the photophysical excitation and emission process of analogues **5**−**17**, we decided to divide the analogues into two moieties. The first moiety is 8-vinyl-adenosine, a known fluorescent nucleoside,[23,24] and the second moiety is a substituted toluene ring, which functions as a fluorescence modulator. We computed the HOMO−LUMO energies of model molecules representing 8-(substituted cinnamyl)-9-Me-adenine moieties: 8-vinyl 9-Me-adenine, **18**, and substituted toluene rings, **19**−**30** (Figure 4). By calculating each part separately, we hoped to achieve a better understanding of the correlation between the toluene ring substituent and the fluorescence of the fluorophore. Moreover, since analogues **5**−**17**, likely undergo an ICT process from the donor moiety to the acceptor moiety, we examined cases in which the 8-vinyl 9-Me-adenine likely plays the donor role and the substituted toluene plays the acceptor role (analogues **5**, **8**−**11**, and **13**−**17**, with the electron-withdrawing group on the toluene ring), and cases in which the 8-vinyl 9-Me-adenine likely plays the acceptor role and the substituted toluene plays the donor role (analogues **6** and **12**, with the electron-donating group on the toluene ring).

Here, HOMO levels of all substituted toluene derivatives, **26**−**29**, had lower energy (−0.266 to −0.334 eV) than that of 8-vinyl-9-Me-adenine, **18**, (−0.253 eV). Moreover, the HOMO−LUMO energy gap of all the analogues was larger ($\Delta E \geq 0.234$ eV) than the energy gap for 8-vinyl-9-Me-adenine, **18**, (0.207 eV), with the exception of analogue **25** with energy gap of 0.191 eV, Table 3. The most interesting results were

Table 3. Molecular Orbital Energies of Compounds 18−30, Obtained from Calculations Run at the M062X/6-311++G(d,p) Level

analogue	substituent	f	HOMO (eV)	LUMO (eV)	Δ (eV)
18	8-vinyl-9-Me-adenine	1.08	−0.253	−0.046	0.207
19	*p*-CF_3	0.81	−0.314	−0.013	0.301
20	*p*-OMe	0.005	−0.266	−0.002	0.264
21	*p*-F	0.03	−0.291	−0.003	0.288
22	*p*-NO_2	0.00	−0.334	−0.094	0.24
23	*p*-CN	0.61	−0.312	−0.032	0.28
24	*p*-COOMe	0.56	−0.317	−0.058	0.259
25	*p*-Me	0.00	−0.272	−0.081	0.191
26	*m*-F	0.28	−0.299	−0.003	0.296
27	*m*-CF_3	0.55	−0.310	−0.018	0.292
28	*m*-NO_2	0.02	−0.330	−0.096	0.234
29	*m*-CN	0.66	−0.310	−0.038	0.272
30	*p*-CN, *m*-CF_3	0.45	−0.314	−0.076	0.238

obtained for the LUMO levels of the analogues. The LUMO levels of all *meta* substituted toluene derivatives, **26**−**29**, were found to have higher energies (from −0.038 to −0.003 eV) than 8-vinyl-9-Me-adenine, **18**, (−0.046 eV) with the exception of nitro-toluene, **28**, which exhibited significantly lower LUMO energy level (−0.096 eV). The *para*-substituted toluene series demonstrates a wide range of LUMO energies (from −0.094 to −0.002 eV) as compared to 8-vinyl-9-Me-adenine's LUMO energy (Table 3). When all LUMO energy levels of all analogues were plotted, we noticed that *meta* or *para* substituted derivatives with LUMO energy level relatively close to LUMO energy of 8-vinyl-9-Me-adenine (−0.076 to −0.003 eV) exhibited high φ values (0.28−0.81), Figure 7.

Figure 8 depicts the HOMO and LUMO orbitals of the unsubstituted compound, **7**, as well as those of *p*- and *m*-NO_2 derivatives **9** and **15**. Inspection of the frontier orbitals of all compounds reveals that the molecular orbitals are delocalized

dx.doi.org/10.1021/jo402050x | J. Org. Chem. 2013, 78, 11999−12008

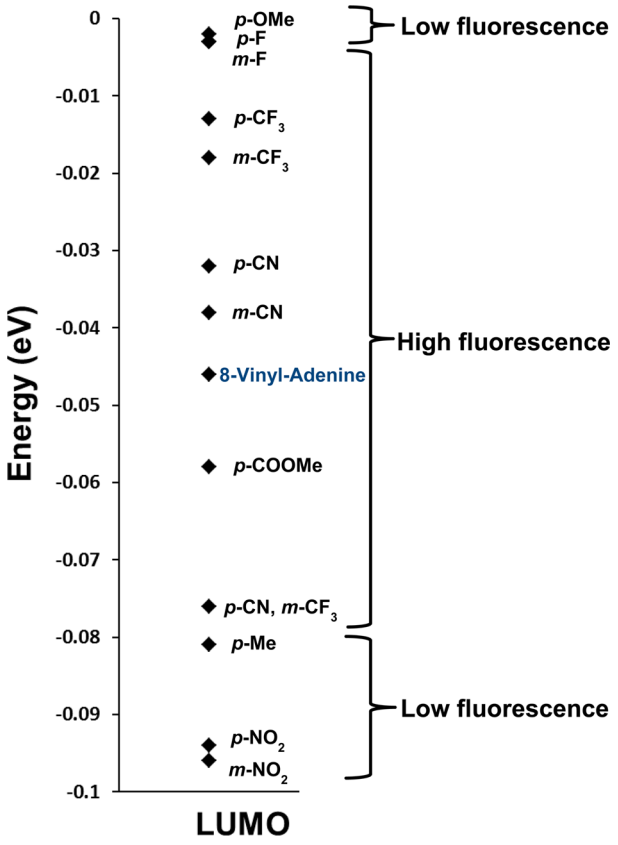

Figure 7. Relationship between LUMO levels of substituted toluene rings, **19**−**30** and 8-vinyl-9-Me-adenine, **18**, and the fluorescent properties of analogues **5**−**17**.

over both rings in most cases, similar to the parent compound (Supporting Information). However, the *p*- and *m*- nitro compounds **9** and **15** are exceptions to this rule. Electron density of the LUMO orbitals of nitro-compounds **9** and **15** is largely localized on the benzene ring, probably due to the strong electron-withdrawing effect of the substituent.

DISCUSSION

We attempted to establish general guidelines that will enable the prediction of fluorescent properties of new nucleoside analogues. For this purpose, we have designed and synthesized C8-extended adenosine analogues **5**−**17**. These 8-(substituted cinnamyl)-adenosine analogues cover a wide chemical space. Indeed, the variously substituted cinnamyl moiety significantly changed the spectral properties (e.g, λ_{abs}, λ_{em}, and φ) of adenosine.

Next, we attempted to correlate quantum yields and emission data with the electronic properties of the cinnamyl moiety in analogues **5**−**17** as reflected by sigma Hammett constants (σ_m or σ_p) of the cinnamyl substituents. Previous reports indicated a linear correlation between sigma values and fluorescent properties of several organic compounds.[32−34] Indeed, here, at sigma values of 0 up to 0.54 for σ_p, or up to 0.56 for σ_m, a linear correlation with the quantum yield was observed. However, at higher or lower σ values no correlation was observed.

Additionally, we sought for a correlation between molecular descriptors (e.g., HOMO−LUMO energies) and fluorescence parameters. The calculated λ_{abs} were in excellent agreement with experimental λ_{abs} indicating that these calculations might be of great use for the prediction of absorption wavelengths of future analogues.

To further our understanding of the influence of the aryl substitution on the fluorescence of analogues **5**−**17**, we studied the electronic effects of the fragments of the 8-cinnamyl-substituted analogues: 8-vinyl-9-Me-adenine, **18**, and substituted toluene rings, **19**−**30**.

A similar computational approach was adopted before for a fluorescein derivative that consists of a donor−acceptor system.[50] Fluorescein was divided into two parts: the xanthene moiety as a fluorophore and the benzene moiety as a fluorescence-controlling moiety, even though there is no obvious structured linker between them. By the division of the molecule and taking advantage of the intramolecular donor−acceptor system, a relationship between the fluorescent quantum yield and the reduction potential of the substituted-benzene moiety was determined.

We observed that the ΔE_{LUMO} between LUMO level of 8-vinyl-9-Me-adenine and LUMO levels of substituted toluene rings is the main factor that determines the quantum yield. This rule applied to analogues in which 8-vinyl-9-Me-adenine played either a donor or acceptor role. Thus, we divide nucleoside analogues, **5**−**17**, into three groups (Table 3, Figure 7): (1) Analogues exhibiting low quantum yields (0.002−0.004) are characterized by low LUMO energy levels (*m*-nitro, **15**, *p*-nitro, **9**, and *p*-Me, **12**, $E \leq -0.081$ eV). (2) Analogues exhibiting high quantum yield (0.28−0.81) are characterized by medium LUMO energy levels (*p*-CN and *m*-CF_3, **17**, *p*-COOMe, **11**, *m*-CN, **16**, *p*-CN, **10**, *m*-CF_3, **14**, *p*-CF_3, **5**, *m*-F, **13**, E −0.076 to −0.003 eV). (3) Analogues exhibiting low quantum yield (0.005 and 0.025) showing high LUMO energy levels (*p*-OMe, **6**, and *p*-F, **8**, $E \geq -0.002$ eV).

In this paper, we examined the influence of the addition of an aryl moiety as a fluorescence modulator, on the fluorescent properties of the fluorophore 8-vinyl-adenosine. The data showed that the emission wavelength of 8-vinyl-adenosine was red-shifted by 31−106 nm, in analogues **5**−**17**, as expected from the elongation of the parent π system. However, for most analogues there was a reduction of the quantum yield upon conjugation of the aryl moiety vs that of the parent compound (0.002−0.61 vs 0.66). The exceptions to this observation were analogue **16**, with *m*-CN substituent, having the same φ value (0.66), and analogue **5**, with *p*-CF_3 substituent, which exhibited a higher φ value (0.81).

In earlier studies, it was found that fluorescence decreases or even disappears upon introduction of a nitro group to fluorescent compounds.[51−53] The mechanism of quenching was related to greatly lowered LUMO energy levels of the aromatic compounds due to the strong electron-withdrawing effect of nitro groups,[54] and this finding is echoed in our results. Indeed, we found that the electron density distribution of the LUMO levels of the nitro analogues, **9** and **15**, are different than that of analogues, **5**−**8**, **10**−**11**, and **16**−**17**. While the other compounds have highly delocalized LUMOs, where the electron density is spread over the entire ring system, in the nitro analogues LUMOs, the electrons are localized mostly on the aryl ring (Figure 8). The localized electron density on the aryl moiety upon excitation causes an electron deficiency in the fluorophore moiety, and a resulting nonradiative pathway with a concomitant fluorescence quenching. This suggests a nearly complete charge-transfer to the aryl group, followed by a very fast recombination pathway, which outcompetes the radiative decay.

dx.doi.org/10.1021/jo402050x | J. Org. Chem. 2013, 78, 11999−12008

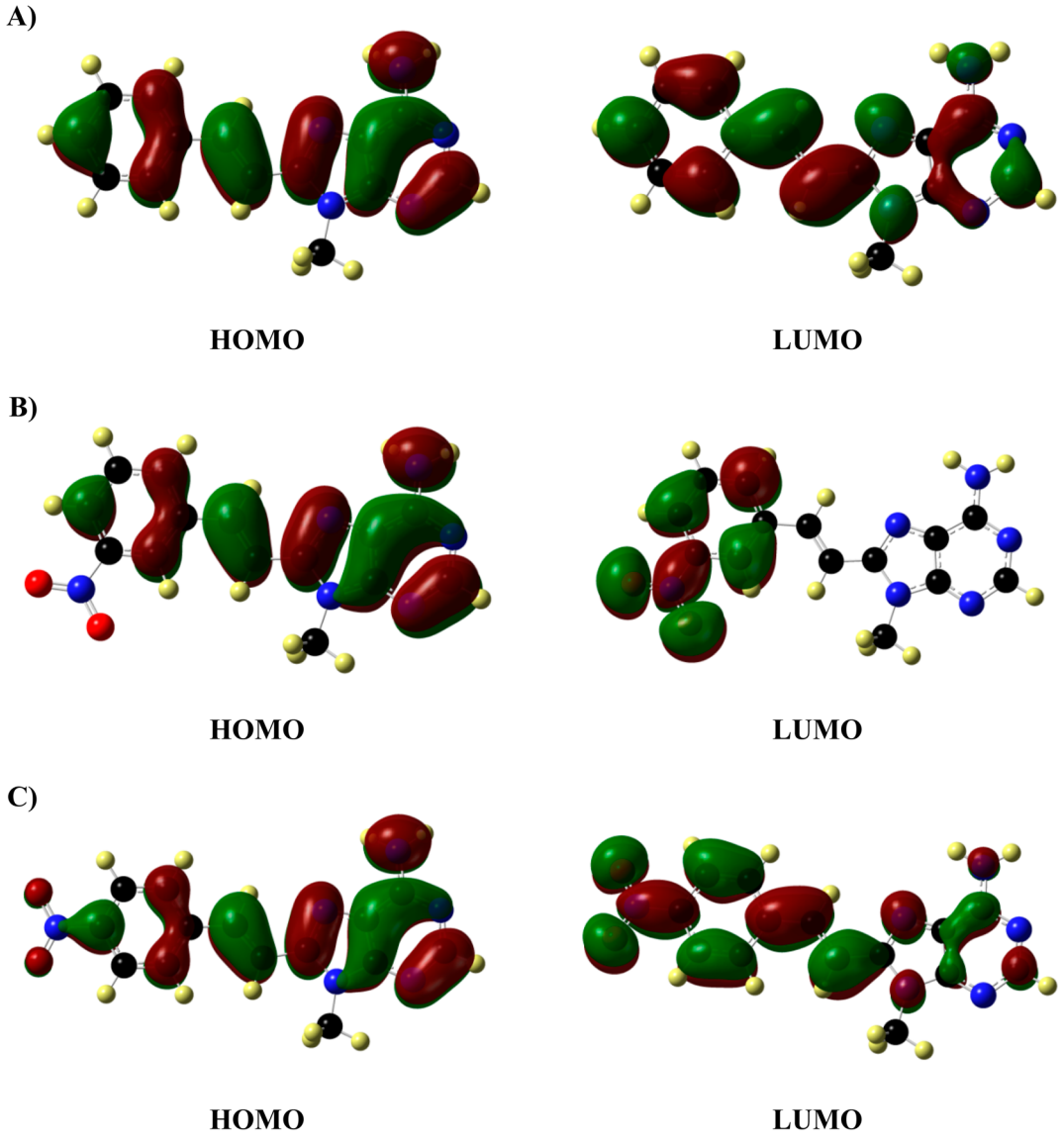

Figure 8. HOMO and LUMO orbitals of analogues **7**, **9**, and **15**. (A) Analogue **7**; (B) Analogue **15**; (C) Analogue **9**.

In conclusion, we reported here on the synthesis and calculations made for a series of 8-(substituted cinnamyl)-adenosine analogues, **5**−**17**. We established a relationship between the ΔE_{LUMO} energy levels of model substituted toluene rings and 8-vinyl-9-Me-adenine and the quantum yields of the corresponding nucleoside analogues. Identification of these relationships between the chemical structure and the fluorescence characteristics of analogues **5**−**17** allows us to design useful fluorescent nucleoside probes. For further development of nucleoside probes based on the scaffold of 8-vinyladenosine moiety, we can expect that only analogues in which the fluorophore modulator moiety exhibits LUMO energy levels within an energy window similar to that of the parent fluorophore will exhibit high φ value.

In addition, we suggested that the quenching character of the nitro group in these analogues is based on their aryl-localized electron density observed in the LUMO orbitals, and hence reduced electron density on the fluorophore, resulting eventually in a nonradiative decay. The correlation identified here constitutes an important tool for the further development of new fluorescent nucleosides to be used in solid phase synthesis for the preparation of hybridization probes, potentially useful for the detection of genetic material.

EXPERIMENTAL SECTION

General Methods. ^{1}H NMR spectra were obtained using a 200, 300, 400, or 600 MHz spectrometer. ^{13}C NMR spectra were obtained at 75, 100, or 150 MHz spectrometer. Chemical shifts are expressed in ppm downfield from Me_4Si (TMS) used as internal standard. The values are given in δ scale. All air and moisture sensitive reactions were carried out in flame-dried, nitrogen flushed flasks sealed with rubber septa, and the reagents were introduced with a syringe. The reactants were dried overnight in a vacuum oven. Progress of the reactions was monitored by TLC on precoated silica gel plates. Visualization was accomplished by UV light. Flash chromatography was carried out on silica gel. Medium pressure chromatography was carried out using automated flash purification system. New compounds were analyzed under ESI (electron spray ionization) conditions on a Q-TOF microinstrument, and high resolution MS-MALDI-TOF spectra were recorded with an autoflex TOF/TOF instrument. Absorption spectra were measured on a UV instrument using a 1 cm path length quartz cell. Emission spectra were measured using luminescence spectrometer, and the emission was corrected for the monochromator sensitivity according to the standard procedure. All commercial

dx.doi.org/10.1021/jo402050x | J. Org. Chem. 2013, 78, 11999−12008

reagents were used without further purification. The fluorescence quantum yield (φ) was determined relative to quinine sulfate in 0.1 M H_2SO_4 (λ_{ex} 350 nm, λ_{em} 446 nm, φ 0.54).[45] Starting materials 8-vinyl adenosine[44] and 8-Br-Adenosine,[43] and analogues **5**,[28] **6**,[28] **7**,[55] and **8**[28] were synthesized according to literature.

DFT Calculations. To elucidate the absorption spectra of the 8-(substituted cinnamyl)-adenosine analogues (SPEC), we performed time-dependent density functional theory (TD-DFT) calculations.[56] The M06-2X functional[57] was employed, as it has been shown to provide excellent agreement with experimental spectra.[58] We note that this global functional is most appropriate for valence and Rydberg excitations, while somewhat less so for charge transfer processes.[59] As a comparison, the absorption spectra computed with the M06HF functional is provided in Table S28 (Supporting Information). All calculations were performed using the polarizable continuum model solvent description modeling MeOH.[60] The TD-DFT calculations were performed using a 6-31+G (d,p) basis set or geometry optimizations of the ground states, while single point calculations used the 6-311++G(3df,2p) basis set.[61] Electronic excitation spectra calculated at the ground state optimized geometry correspond to the absorption spectra. In addition to the absorption wavelengths, oscillator strengths were computed, to provide information regarding the intensity of the electronic transitions. All calculations used the Gaussian 09 program.[62]

General Procedure for the Preparation of Analogues 9−11 and 14−17.[42] A mixture of $Pd(OAc)_2$ (4 mg, 0.02 mmol), P(*o*-tol)$_3$ (10.2 mg, 0.03 mmol), Et_3N (111 μL, 0.8 mmol), 8-vinyladenosine (50 mg, 0.17 mmol), and aryl bromide/aryl iodide (0.34 mmol) in DMF (2 mL) was prepared in an oven-dried vial, equipped with a stirring bar, and was heated to 100−105 °C. Although the general procedure described is for reactions on the 50 mg scale of 8-vinyladenosine, some reactions were conducted at different scales, and in these cases the proportions of reagents and solvents were appropriately adjusted. Reactions were monitored by TLC, and upon consumption of the starting material, the reaction mixtures were diluted with EtOAc (40 mL) and washed with brine (20 mL) and water (40 mL). The organic layer was separated, dried over Na_2SO_4, and concentrated. The crude reaction products were purified by silica gel column chromatography using DCM:MeOH (98:2−95:5) or EtOAc:MeOH (98:2) as the eluent.

*2-(6-Amino-8-(4-nitrostyryl)-9H-purin-9-yl)-5-(hydroxymethyl)-tetrahydrofuran-3,4-diol (**9**).* Product **9** was obtained as a dark brown solid (20 mg, 28%), starting from 8-vinyladenosine (50 mg, 0.1706 mmol) and 4-bromonitrobenzene (69 mg, 0.34 mmol): mp 198 °C (dec); ^{1}H NMR (600 MHz, DMSO-d_6) δ 8.25 (d, J = 9 Hz, 2H), 8.13 (s, 1H), 8.03 (d, J = 9 Hz, 2H), 7.84 (s, 2H), 7.46 (s, 2H), 6.17 (d, J = 7.2 Hz, 1H), 5.82 (dd, J = 7.8 and 3.6 Hz, 1H), 5.35 (d, J = 7.2 Hz, 1H), 5.26 (d, J = 4.8 Hz, 1H), 4.71 (q, J = 7.2 Hz, 1H), 4.21 (m, 1H), 4.04 (m, 1H), 3.74 (m, 1H), 3.64 (m, 1H) ppm; ^{13}C NMR (150 MHz, DMSO-d_6) δ 155.9, 152.4, 150.2, 147.3, 147.1, 142.3, 133.6, 128.5, 124.1, 119.43, 119.40, 87.5, 86.5, 73.0, 70.4, 61.8 ppm; UV−vis (CH_3OH) λ_{max} 367 nm; HRMS (MALDI) m/z calcd for $C_{18}H_{19}N_6O_6$ $[M + H]^+$ 415.1361, found 415.1360.

*4-((E)-2-(6-Amino-9-(3,4-dihydroxy-5-(hydroxymethyl)-tetrahydrofuran-2-yl)-9H-purin-8-yl)vinyl)benzonitrile (**10**).* Product **10** was obtained as a yellow solid (20 mg, 30%), starting from 8-vinyladenosine (50 mg, 0.1706 mmol) and 4-iodobenzonitrile (78 mg, 0.34 mmol): mp 219 °C (dec); ^{1}H NMR (200 MHz, DMSO-d_6) δ 8.12 (s, 1H), 7.97 (d, J = 8.4 Hz, 2H), 7.87 (d, J = 8.4 Hz, 2H), 7.78 (s, 2H), 7.46 (s, 2H), 6.16 (d, J = 7.4 Hz, 1H), 5.82 (dd, J = 7.2 and 3.2 Hz, 1H), 5.35 (d, J = 7.2 Hz,1H), 5.25 (d, J = 4.4 Hz, 1H), 4.71 (m, 1H), 4.20 (m, 1H), 4.03 (m, 1H), 3.74−3.62 (m, 2H) ppm; ^{13}C NMR (75 MHz, DMSO-d_6) δ 156.3, 152.7, 150.6, 147.9, 140.7, 134.7, 133.2, 128.7,119.8, 119.3, 119.0, 111.3, 88.1, 87.0, 73.3, 70.9, 62.3 ppm; UV−vis (CH_3OH) λ_{max} 350 nm; HRMS (MALDI) m/z calcd for $C_{19}H_{19}N_6O_4$ $[M + H]^+$ 395.1462, found 395.1470.

*Methyl 4-((E)-2-(6-amino-9-(3,4-dihydroxy-5-(hydroxymethyl)-tetrahydrofuran-2-yl)-9H-purin-8-yl)vinyl)benzoate (**11**).* Product **11** was obtained as a brown solid (25 mg, 35%), starting from 8-vinyladenosine (50 mg, 0.1706 mmol) and methyl 4-bromobenzoate (74 mg, 0.34 mmol): mp 218 °C (dec); ^{1}H NMR (300 MHz, DMSO-d_6) δ 8.12 (s, 1H), 7.99 (d, J = 8.4 Hz, 2H), 7.90 (d, J = 8.4 Hz, 2H), 7.81 (d, J = 15.3 Hz, 1H), 7.73 (d, J = 15.3 Hz, 1H), 7.44 (s, 2H), 6.16 (d, J = 7.2 Hz, 1H), 5.82 (dd, J = 7.8 and 3.6 Hz, 1H), 5.36 (m, 1H), 5.27 (m, 1H), 4.73 (m, 1H), 4.21 (m, 1H), 4.03 (m, 1H), 3.87 (s, 3H), 3.77−3.60 (m, 2H) ppm; ^{13}C NMR (75 MHz, DMSO-d_6) δ165.9, 155.8, 152.1, 150.1, 147.6, 140.2, 134.7, 129.6, 129.5, 127.7, 119.3, 117.6, 87.5, 86.5, 72.8, 70.4, 61.8, 52.2 ppm; UV−vis (CH_3OH) λ_{max} 342 nm; HRMS (MALDI) m/z calcd for $C_{20}H_{22}N_5O_6$ $[M + H]^+$ 428.1565, found 428.1560.

*2-(6-Amino-8-(3-(trifluoromethyl)styryl)-9H-purin-9-yl)-5-(hydroxymethyl)tetrahydrofuran-3,4-diol (**14**).* Product **14** was obtained as a light brown solid (56 mg, 47%), starting from 8-vinyladenosine (80 mg, 0.27 mmol) and 3-bromobenzotrifluoride (123 mg, 0.54 mmol): mp 211 °C (dec); ^{1}H NMR (600 MHz, DMSO-d_6) δ 8.17 (s, 1H), 8.12 (s, 1H), 8.03 (d, J = 7.5 Hz, 1H), 7.81 (d, J = 15 Hz, 1H), 7.75 (d, J = 15 Hz, 1H), 7.71 (d,J = 7.5 Hz, 1H), 7.66 (t, J = 7.5 Hz, 1H), 7.41 (s, 2H), 6.17 (d, J = 7.2 Hz, 1H), 5.78 (dd, J = 8.4 and 4.2 Hz, 1H), 5.34 (d, J = 7.2 Hz, 1H), 5.22 (d, J = 4.8 Hz, 1H), 4.76 (q, J = 7.2 Hz, 1H), 4.22 (m, 1H), 4.03 (m, 1H), 3.73 (m, 1H), 3.63 (m, 1H) ppm; ^{13}C NMR (150 MHz, DMSO-d_6) δ 155.8, 152.0, 150.0, 147.7, 136.8, 134.6, 131.6, 130.1, 129.9, 129.7, 129.5, 126.8, 125.3, 125.3, 125.0, 123.8, 123.7, 123.2, 121.4, 119.3, 116.9, 87.7, 86.6, 72.7, 70.5, 61.9 ppm; UV−vis (CH_3OH) λ_{max} 334 nm; HRMS (MALDI) m/z calcd for $C_{19}H_{18}F_3N_5NaO_4$ $[M + H]^+$ 460.1203, found 460.1230.

*2-(6-Amino-8-(3-nitrostyryl)-9H-purin-9-yl)-5-(hydroxymethyl)-tetrahydrofuran-3,4-diol (**15**).* Product **15** was obtained as a brown solid (20 mg, 18%), starting from 8-vinyladenosine (80 mg, 0.273 mmol) and 1-bromo-3-nitrobenzene (111 mg, 0.546 mmol): mp 188 °C (dec); ^{1}H NMR (600 MHz, DMSO-d_6) δ 8.61 (s, 1H), 8.20 (d, J = 8.4 Hz, 2H), 8.12 (s, 1H), 7.85 (d, J = 16.2 Hz, 1H), 7.81 (d, J = 16.2 Hz, 1H), 7.71 (t, J = 8.4 Hz, 1H), 7.43 (s, 2H), 6.18 (d, J = 7.2 Hz, 1H), 5.79 (dd, J = 7.8 and 3.6 Hz, 1H), 5.35 (m, 1H), 5.25 (m, 1H), 4.76 (m, 1H), 4.21 (m, 1H), 4.04 (m, 1H), 3.74 (m, 1H), 3.63(m, 1H) ppm; ^{13}C NMR (150 MHz, DMSO-d_6) δ 155.8, 152.1, 150.0, 148.5, 147.5, 137.5, 133.8, 130.3, 123.3, 121.7, 121.6, 119.3, 117.9, 87.7, 86.6, 72.7, 70.5, 61.9 ppm; UV−vis (CH_3OH) λ_{max} 335 nm; HRMS (MALDI) m/z calcd for $C_{18}H_{18}N_6O_6Na$ $[M + Na]^+$ 437.1186, found 437.1184.

*3-((E)-2-(6-Amino-9-(3,4-dihydroxy-5-(hydroxymethyl)-tetrahydrofuran-2-yl)-9H-prin-8-yl)vinyl)benzonitrile (**16**).* Product **16** was obtained as a brown solid (11 mg, 10%), starting from 8-vinyladenosine (80 mg, 0.273 mmol) and 3-bromobenzonitrile (100 mg, 0.546 mmol): mp 177 °C; ^{1}H NMR (600 MHz, DMSO-d_6) δ 8.31 (s, 1H), 8.11 (s, 1H), 8.07 (d, J = 7.8 Hz, 1H), 7.81 (d, J = 7.8 Hz, 1H), 7.74 (s, 2H), 7.63 (t, J = 7.8 Hz, 1H), 7.42 (s, 2H), 6.16 (d, J = 7.2 Hz, 1H), 5.81 (dd, J = 8.4 and 4.2 Hz, 1H), 5.32 (d, J = 6.6 Hz, 1H), 5.23 (d, J = 4.2 Hz, 1H), 4.75 (m, 1H), 4.22 (m, 1H), 4.03 (m, 1H), 3.73 (m, 1H), 3.63 (m, 1H) ppm; ^{13}C NMR (150 MHz, DMSO-d_6) δ 155.8, 152.1, 150.0, 147.5, 136.9, 133.9, 132.2, 132.1, 130.7, 130.0, 119.3, 118.6, 117.3, 112.1, 87.7, 86.6, 72.7, 86.6, 72.7, 70.4, 61.9 ppm; UV−vis (CH_3OH) λ_{max} 337 nm; HRMS (MALDI) m/z calcd for $C_{19}H_{19}N_6O_4$ $[M + H]^+$ 395.1468, found 395.1475.

*4-((E)-2-(6-Amino-9-((2R,3R,4S,5R)-3,4-dihydroxy-5-(hydroxymethyl)tetrahydrofuran-2-yl)-9H-purin-8-yl)vinyl)-2-(trifluoromethyl)benzonitrile (**17**).* Product **17** was obtained as a yellow solid (55 mg, 35%), starting from 8-vinyladenosine (100 mg, 0.341 mmol) and 4-bromo-2-(trifluoromethyl)benzonitrile (171 mg, 0.682 mmol): mp 236 °C (dec); ^{1}H NMR (600 MHz, DMSO-d_6) δ 8.42 (s, 1H), 8.22 (d, J = 7.8 Hz, 1H), 8.18 (d, J = 7.8 Hz, 1H), 8.13 (s, 1H), 7.95 (d, J = 15.6 Hz, 1H), 7.85 (d, J = 15.6 Hz, 1H), 7.46 (s, 2H), 6.19 (d, J = 7.2 Hz, 1H), 5.77 (dd, J = 7.5 and 3 Hz, 1H), 5.34 (d, J = 6.6 Hz, 1H), 5.24 (d, J = 4.2 Hz, 1H), 4.74 (m, 1H), 4.22 (m, 1H), 4.04 (m, 1H), 3.73(m, 1H), 3.64 (m, 1H) ppm; ^{13}C NMR (150 MHz, DMSO-d_6) δ 156.0, 152.4, 150.1, 147.1, 141.1, 135.8, 132.9, 131.8, 131.5, 131.3, 131.1, 125.42, 125.39, 125.3, 123.5, 121.7, 120.4, 119.8, 119.5, 115.7, 87.7, 86.6, 72.9, 70.4, 61.9 ppm; UV−vis (CH_3OH) λ_{max} 356 nm; HRMS (MALDI) m/z calcd for $C_{20}H_{18}N_6O_4F_3$ $[M + H]^+$ 463.1342, found 463.1345.

General Procedure for the Preparation of Analogues 5–8 and 12–13.[40,41] Water–acetonitrile (2:1, 3 mL) mixture was added through a septum to an argon-purged round-bottom flask containing 8-bromo-adenosine (0.29 mmol, 1 equiv), $Pd(OAc)_2$ (0.011 mmol, 0.05 equiv), sodium carbonate (0.87 mmol, 3 equiv), tris(3-sulfonatophenyl) phosphine trisodium salt (Tppts) (0.072 mmol, 0.25 equiv), and the appropriate boronic acid derivative (0.36 mmol, 1.25 equiv). The mixture was stirred at 90 °C under argon atmosphere for ∼2 h. The reaction was cooled to room temperature, and few drops of 37% HCl were added (up to pH∼7). The product was purified on a silica gel column using $CHCl_3$:MeOH (98:2–94:6) as the eluent.

*2-(6-Amino-8-((E)-4-methylstyryl)-9H-purin-9-yl)-5-(hydroxymethyl)tetrahydrofuran-3,4-diol (**12**).* Product **12** was obtained as a light yellow solid (30 mg, 27%), starting from 8-bromo-adenosine (100 mg, 0.289 mmol) and trans-2-(4-methylphenyl)vinylboronic acid (59 mg, 0.36 mmol): mp 213 °C (dec); ^{1}H NMR (400 MHz, DMSO-d_6) δ 8.09 (s, 1H), 7.72 (d, J = 15.4 Hz, 1H), 7.65 (d, J = 7.6 Hz, 2H), 7.48 (d, J = 15.4 Hz, 1H), 7.36 (s, 2H), 7.24 (d, J = 7.6 Hz, 2H), 6.11 (d, J = 6.8 Hz, 1H), 5.80 (m, 1H), 5.33 (d, J = 6.8 Hz, 1H), 5.22 (d, J = 4.2 Hz, 1H), 4.76 (m, 1H), 4.20 (m, 1H), 4.02 (m, 1H), 3.73 (m, 1H), 3.61 (m, 1H), 2.34 (s, 3H) ppm; ^{13}C NMR (150 MHz, DMSO-d_6) δ 155.6, 151.7, 149.9, 148.3, 138.8, 136.3, 132.9, 129.5, 127.5, 119.2, 113.6, 87.6, 86.5, 72.6, 70.5, 61.8, 21.0 ppm; UV–vis (CH_3OH) λ_{max}338 nm; HRMS (MALDI) m/z calcd for $C_{19}H_{22}N_5O_4$ $[M + H]^+$ 384.1672, found 384.1669.

*2-(6-Amino-8-(3-fluorostyryl)-9H-purin-9-yl)-5-(hydroxymethyl)-tetrahydrofuran-3,4-diol (**13**).* Product **13** was obtained as a white solid (39 mg, 35%), starting from 8-bromo-adenosine (100 mg, 0.289 mmol) and trans-2-(3-fluorophenyl)vinylboronic acid (60 mg, 0.36 mmol): mp 265 °C (dec); ^{1}H NMR (300 MHz, DMSO-d_6) δ 8.11 (s, 1H), 7.74 (d, J = 15.9 Hz, 1H), 7.64 (d, J = 15.9 Hz, 1H), 7.69 (m, 1H), 7.56 (m, 1H), 7.46 (m, 1H), 7.43 (s, 2H), 7.2 (m, 1H), 6.15 (d, J = 7.2 Hz, 1H), 5.84 (dd, J = 8.1 and 3.9 Hz, 1H), 5.34 (d, J = 6.5 Hz, 1H), 5.26 (d, J = 3.9 Hz, 1H), 4.73 (m, 1H), 4.21 (m, 1H), 4.03 (m, 1H), 3.76–3.71 (m, 1H), 3.66–3.64 (m, 1H) ppm; ^{13}C NMR (100 MHz, DMSO-d_6) δ 162.5, 155.7, 151.9, 150.4, 149.9, 147.7, 138.1, 134.8, 130.7, 124.1, 119.2, 116.3, 115.7, 113.3, 87.6, 86.5, 72.7, 70.3, 61.8 ppm; UV–vis (CH_3OH) λ_{max} 336 nm; HRMS (MALDI) m/z calcd for $C_{18}H_{19}FN_5O_4$ $[M + H]^+$ 388.1416, found 388.1420.

■ ASSOCIATED CONTENT

Supporting Information

^{13}C and ^{1}H NMR spectra of reported analogues, fluorescence spectra for selected analogues, and theoretical data. This material is available free of charge via the Internet at http://pubs.acs.org.

■ AUTHOR INFORMATION

Corresponding Author

*Fax: 972-3-6354907. Tel.: 972-3-5318303. E-mail: bilha.fischer@biu.ac.il.

Notes

The authors declare no competing financial interest.

■ REFERENCES

(1) Namba, K.; Osawa, A.; Ishizaka, S.; Kitamura, N.; Tanino, K. *J. Am. Chem. Soc.* **2011**, *133*, 11466–11469.
(2) Kricka, L. J.; Fortina, P. *Clin. Chem.* **2009**, *55*, 670–683.
(3) Shinar, J. *Organic Light-Emitting Devices*; Springer: New York, 2004.
(4) Valeur, B. *Molecular Fluorescence: Principles and Applications*; Wiley-VCH: Weinheim, 2002.
(5) Nir, E.; Kleinermanns, K.; Grace, L.; de Vries, M. S. *J. Phys. Chem. A* **2001**, *105*, 5106–5110.
(6) Callis, P. R. *Annu. Rev. Phys. Chem.* **1983**, *34*, 329–357.
(7) Daniels, M.; Hauswirth, W. *Science* **1971**, *171*, 675–677.
(8) Udenfriend, S.; Zaltzman, P. *Anal. Biochem.* **1962**, *3*, 49–59.
(9) Gallardo-Escarate, C.; Alvarez-Borrego, J.; Von, B. E.; Dupre, E.; Del, R.-P. M. A. *Biol. Res.* **2007**, *40*, 29–40.
(10) Milanovich, N.; Suh, M.; Jankowiak, R.; Small, G. J.; Hayes, J. M. *J. Phys. Chem.* **1996**, *100*, 9181–9186.
(11) Milanovich, N.; Hayes, J. M.; Small, G. J. *Mol. Cryst. Liq. Cryst. Sci. Technol., Sect. A* **1996**, *291*, 147–154.
(12) Pribylova, R.; Kralik, P.; Pavlik, I. *Mol. Biotechnol.* **2009**, *42*, 30–40.
(13) Arvey, A.; Hermann, A.; Hsia, C. C.; Ie, E.; Freund, Y.; McGinnis, W. *Nucleic Acids Res.* **2010**, *38*, e115/111–e115/117.
(14) Wabuyele, M. B.; Soper, S. A. *Single Mol.* **2001**, *2*, 13–21.
(15) Ramshesh, V. K.; Knisley, S. B. *J. Biomed. Opt.* **2006**, *11*, 024019.
(16) Wilhelmsson, L. M.; Holmen, A.; Lincoln, P.; Nielsen, P. E.; Norden, B. *J. Am. Chem. Soc.* **2001**, *123*, 2434–2435.
(17) Wahba, A. S.; Damha, M. J.; Hudson, R. H. E. *Nucleic Acids Symp. Ser.* **2008**, *52*, 399–400.
(18) Hudson, R. H. E.; Ghorbani-Choghamarani, A. *Synlett* **2007**, 870–873.
(19) Sinkeldam, R. W.; Tor, Y. *Collect. Symp. Ser.* **2011**, *12*, 101–107.
(20) Sinkeldam, R. W.; Wheat, A. J.; Boyaci, H.; Tor, Y. *ChemPhysChem* **2011**, *12*, 567–570.
(21) Dodd, D. W.; Hudson, R. H. E. *Mini-Rev. Org. Chem.* **2009**, *6*, 378–391.
(22) Hudson, R. H. E.; Moszynski, J. M. *Synlett* **2006**, 2997–3000.
(23) Ben, G. N.; Glasser, N.; Ramalanjaona, N.; Beltz, H.; Wolff, P.; Marquet, R.; Burger, A.; Mely, Y. *Nucleic Acids Res.* **2005**, *33*, 1031–1039.
(24) Kodali, G.; Kistler, K. A.; Narayanan, M.; Matsika, S.; Stanley, R. J. *J. Phys. Chem. A* **2010**, *114*, 256–267.
(25) Sharon, E.; Levesque, S. A.; Munkonda, M. N.; Sevigny, J.; Ecke, D.; Reiser, G.; Fischer, B. *ChemBioChem* **2006**, *7*, 1361–1374.
(26) Major, D. T.; Fischer, B. *J. Phys. Chem. A* **2003**, *107*, 8923–8931.
(27) Noe, M. S.; Rios, A. C.; Tor, Y. *Org. Lett.* **2012**, *14*, 3150–3153.
(28) Zilbershtein, L.; Silberman, A.; Fischer, B. *Org. Biomol. Chem.* **2011**, *9*, 7763–7773.
(29) McClure, D. S. *J. Chem. Phys.* **1949**, *17*, 905–913.
(30) Takadate, A.; Masuda, T.; Murata, C.; Isobe, A.; Shinohara, T.; Irikura, M.; Goya, S. *Anal. Sci.* **1997**, *13*, 753–756.
(31) Matsunaga, H.; Santa, T.; Iida, T.; Fukushima, T.; Homma, H.; Imai, K. *Analyst* **1997**, *122*, 931–936.
(32) Cheshmedzhieva, D.; Ivanova, P.; Stoyanov, S.; Tasheva, D.; Dimitrova, M.; Ivanov, I.; Ilieva, S. *Phys. Chem. Chem. Phys.* **2011**, *13*, 18530–18538.
(33) Sherman, W. R.; Robins, E. *Anal. Chem.* **1968**, *40*, 803–805.
(34) Uchiyama, S.; Santa, T.; Suzuki, S.; Yokosu, H.; Imai, K. *Anal. Chem.* **1999**, *71*, 5367–5371.
(35) Butler, R. S.; Cohn, P.; Tenzel, P.; Abboud, K. A.; Castellano, R. K. *J. Am. Chem. Soc.* **2009**, *131*, 623–633.
(36) Butler, R. S.; Myers, A. K.; Bellarmine, P.; Abboud, K. A.; Castellano, R. K. *J. Mater. Chem.* **2007**, *17*, 1863–1865.
(37) Haidekker, M. A.; Theodorakis, E. A. *J. Biol. Eng.* **2010**, *4*, 11.
(38) Kumar Paul, B.; Samanta, A.; Kar, S.; Guchhait, N. *J. Lumin.* **2010**, *130*, 1258–1267.
(39) Nandy, R.; Sankararaman, S. *Beilstein J. Org. Chem.* **2010**, *6*, 992–1001 No. 1112.
(40) Collier, A.; Wagner, G. K. *Synth. Commun.* **2006**, *36*, 3713–3721.
(41) Capek, P.; Pohl, R.; Hocek, M. *Org. Biomol. Chem.* **2006**, *4*, 2278–2284.
(42) Lagisetty, P.; Zhang, L.; Lakshman, M. K. *Adv. Synth. Catal.* **2008**, *350*, 602–608.
(43) Butora, G.; Schmitt, C.; Levorse, D. A.; Streckfuss, E.; Doss, G. A.; MacCoss, M. *Tetrahedron* **2007**, *63*, 3782–3789.
(44) Mamos, P.; Van Aerschot, A. A.; Weyns, N. J.; Herdewijn, P. A. *Tetrahedron Lett.* **1992**, *33*, 2413–2416.
(45) Yvon, J. *A Guide to recording fluorescence quantum yields*. http://www.jobinyvon.com.

(46) Lakowicz, J. R. *Principles of Fluorescent Spectroscopy*; Springer: Baltimore, MD, 1986.
(47) McDaniel, D. S.; Brown, H. C. *J. Org. Chem.* **1958**, *23*, 420−427.
(48) Charton, M. *Prog. Phys. Org. Chem.* **1981**, *13*, 119−251.
(49) Yi, S.; Men, J.; Wu, D.; Yang, M.; Sun, H.; Chen, H.; Gao, G. *Des. Monomers Polym.* **2011**, *14*, 367−381.
(50) Ueno, T.; Urano, Y.; Setsukinai, K.; Takakusa, H.; Kojima, H.; Kikuchi, K.; Ohkubo, K.; Fukuzumi, S.; Nagano, T. *J. Am. Chem. Soc.* **2004**, *126*, 14079−14085.
(51) Seely, G. R. *J. Phys. Chem.* **1969**, *73*, 125−129.
(52) Motoyoshiya, J.; Fengqiang, Z.; Nishii, Y.; Aoyama, H. *Spectrochim. Acta, Part A* **2008**, *69A*, 167−173.
(53) Jian, C.; Seitz, W. R. *Anal. Chim. Acta* **1990**, *237*, 265−271.
(54) Ueno, T.; Urano, Y.; Kojima, H.; Nagano, T. *J. Am. Chem. Soc.* **2006**, *128*, 10640−10641.
(55) Kohyama, N.; Katashima, T.; Yamamoto, Y. *Synthesis* **2004**, 2799−2804.
(56) Bauernschmitt, R.; Ahlrichs, R. *Chem. Phys. Lett.* **1996**, *256*, 454−464.
(57) Zhao, Y.; Truhlar, D. G. *Theor. Chem. Acc.* **2008**, *120*, 215−241.
(58) Isegawa, M.; Peverati, R.; Truhlar, D. G. *J. Chem. Phys.* **2012**, *137*, 244104.
(59) Jacquemin, D.; Perpete, E. A.; Ciofini, I.; Adamo, C.; Valero, R.; Zhao, Y.; Truhlar, D. G. *J. Chem. Theory Comput.* **2010**, *6*, 2071−2085.
(60) Tomasi, J.; Mennucci, B.; Cammi, R. *Chem. Rev.* **2005**, *105*, 2999−3094.
(61) Hehre, W. J. *Acc. Chem. Res.* **1976**, *9*, 399−406.
(62) Frisch, M. J.; Trucks, G. W.; Schlegel, H. B.; Scuseria, G. E.; Robb, M. A.; Cheeseman, J. R.; Scalmani, G.; Barone, V.; Mennucci, B.; Petersson, G. A.; Nakatsuji, H.; Caricato, M.; Li, X.; Hratchian, H. P.; Izmaylov, A. F.; Bloino, J.; Zheng, G.; Sonnenberg, J. L.; Hada, M.; Ehara, M.; Toyota, K.; Fukuda, R.; Hasegawa, J.; Ishida, M.; Nakajima, T.; Honda, Y.; Kitao, O.; Nakai, H.; Vreven, T.; Montgomery, J. A., Jr.; Peralta, J. E.; Ogliaro, F.; Bearpark, M.; Heyd, J. J.; Brothers, E.; Kudin, K. N.; Staroverov, V. N.; Kobayashi, R.; Normand, J. ; Raghavachari, K.; Rendell, A.; Burant, J. C.; Iyengar, S. S.; Tomasi, J.; Cossi, M.; Rega, N.; Millam, J. M.; Klene, M.; Knox, J. E.; Cross, J. B.; Bakken, V.; Adamo, C.; Jaramillo, J.; Gomperts, R.; Stratmann, R. E.; Yazyev, O. ; Austin, A. J.; Cammi, R.; Pomelli, C.; Ochterski, J. W.; Martin, R. L.; Morokuma, K.; Zakrzewski, V. G.; Voth, G. A.; Salvador, P.; Dannenberg, J. J.; Dapprich, S.; Daniels, A. D. Farkas, J.; Foresman, B.; Ortiz, J. V.; Cioslowski, J.; Fox, D. J. *Gaussian 09*; Gaussian, Inc.: Wallingford, CT, 2009.